Hydrogeologic characterization of a groundwater system using sequential aquifer tests and flowmeter logs

Stephen G. Mclin

2007, pp. 485-491. https://doi.org/10.56577/FFC-58.485

in:

Geology of the Jemez Region II, Kues, Barry S., Kelley, Shari A., Lueth, Virgil W.; [eds.], New Mexico Geological Society 58 th Annual Fall Field Conference Guidebook, 499 p. https://doi.org/10.56577/FFC-58

This page is intentionally left blank to maintain order of facing pages.

HYDROGEOLOGIC CHARACTERIZATION OF A GROUNDWATER SYSTEM USING SEQUENTIAL AQUIFER TESTS AND FLOWMETER LOGS

STEPHEN G. MCLIN
Los Alamos National Laboratory, P.O. Box 1663, Los Alamos, NM 87545, sgm@lanl.gov

Abstract — Four sequential aquifer tests were conducted in new municipal water supply wells located in Guaje Canyon on the northeastern flank of Pajarito Plateau. The plateau borders the western perimeter of the Española Basin and defines the western margin of the Rio Grande rift system. Each aquifer test consisted of a pumping and recovery phase, and adjacent wells were used to record both drawdown and recovery data. Collectively, these tests reveal horizontal propagation of drawdown in the regional aquifer beyond about 2500-4800 ft from individual pumping wells. Each well is approximately 2000 ft deep, and has about 1300 ft of continuous louvered screen at the bottom. However, dynamic flowmeter logs from each well show an effective aquifer thickness (or high water-yielding interval) that is only about 435 ft in the east and thins to about 325 ft in the west over a lateral distance of about 8300 ft. These logs demonstrate that the aquifer is highly stratified and laterally discontinuous. In the east, this high-yielding interval is located above the Miocene basalt flows that separate poorly sorted, fluvial Santa Fe Group deposits from lower yielding fine-grained sandstone and siltstones. In the west, this high-yielding interval is interbedded with the basalts. Aquifer transmissivity varies from about 3440 ft^2/day in the east to about 700 ft^2/day in the west. This westward decline in transmissivity is strongly correlated to the observed westward thinning of the high-yielding interval so hydraulic conductivity remains nearly constant. The storage coefficient averaged about 0.00062 for the four aquifer tests and is characteristic of early-time confined behavior. Complex barrier, or no-flow, boundary effects are also apparent after several hundred minutes of pumping and mask the theoretical transition from a confined to phreatic aquifer response. Mesa-top surface expressions of faulting were mapped in the Puye Quadrangle by Dethier (2003); here, several of his fault traces are projected into the alluvial canyon drainage system where the well field is located. These projections coincide with predicted locations of buried, no-flow boundaries obtained from aquifer test analyses. These results imply that aquifer units not only thin to the west but are also displaced vertically downward by normal faulting as one moves to the east and toward the floor of the Rio Grande rift system.

SITE LOCATION AND TEST DESCRIPTION

The Guaje well field is located in Guaje Canyon on the northeastern flank of Pajarito Plateau (Fig.1). Historically, the highest yielding water supply wells have been located in the east-central plateau area and penetrate into relatively thick sequences of the Puye fanglomerate where axial deposits of ancestral Rio Grande gravels (i.e., the Totavi Lentil of Griggs, 1964) are commonly encountered (Purtymun, 1984; Purtymun and Stoker, 1988; Broxton and Vaniman, 2005). This east-central portion of the regional

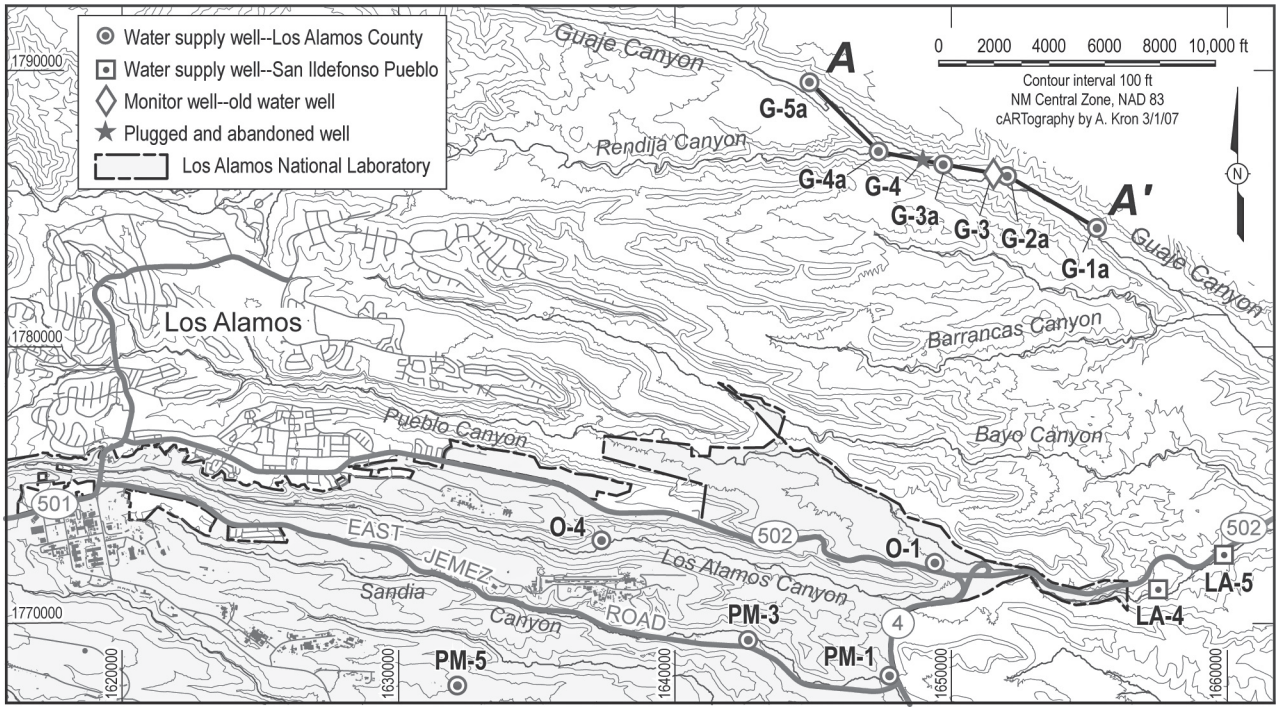

FIGURE 1. Location of wells on Pajarito Plateau. Note the location of cross-section A-A' in Guaje Canyon.

aquifer is the primary source of potable drinking water for Los Alamos County, Los Alamos National Laboratory, and Bandelier National Monument; it has been described by numerous authors (e.g., Purtymun and Johansen, 1974; Purtymun, 1995; Broxton and Reneau, 1996; McLin, 2005a, 2006a; Collins et al., 2006). In contrast, the Guaje well field is less productive and shows more drawdown than other water supply wells located in the east-central plateau area (e.g., McLin, 2006b, c). The Guaje Canyon area has been described by Purtymun (1995), Reneau and Dethier (1996), Shomaker (1999), Dethier (2003), and WoldeGabriel et al. (2006).

Four sequential aquifer tests were conducted in the Guaje well field shortly after four new replacement wells were installed in 1998 (McLin, 2006b). Each test consisted of pumping a single well at a constant discharge rate and observing water level changes in both the pumping and surrounding observation wells. During each test cycle, a two-day pumping interval was followed by a two-day recovery period. Individual test cycles were separated by at least 30 days of nonpumping and allowed for nearly complete water level recovery. The purpose of these tests was to estimate aquifer parameters that characterize the saturated porous media below Guaje Canyon. These parameters include aquifer transmissivity (T), storage coefficient (S), and thickness (b). Traditionally, T and S are obtained from aquifer tests while $\underline{b}$ is estimated from drilling and/or geophysical logs (e.g., Fetter, 1994). Hydraulic conductivity (K) is then determined after dividing T by b, while specific storage (S_s) is determined after dividing S by b. This traditional approach assumes that $\underline{b}$ can be accurately identified using lithology and is rarely confirmed by alternate methods. In this study, dynamic flowmeter logs were used to make direct hydraulic measurements of b (e.g., Izbicki et al., 2005). A secondary test objective was to identify any recharge or barrier boundary effects that might be located near the well field.

Hydrogeologic cross-section A-A' (Fig. 2) runs west to east through the Guaje well field, and is based on recent work by Shomaker (1999), McLin (2006b), and WoldeGabriel et al. (2006). This cross-section represents a complex regional aquifer system that consists of several distinct hydrostratigraphic zones that yield substantially different volumetric flow rates over the vertical screened interval of each production well. As shown below, these hydrostratigraphic zones do not precisely correlate with previously identified stratigraphic units. Each well is hydraulically dominated by water produced from poorly sorted, medium- to fine-grained, arkosic sandstones and interbedded siltstones from the Miocene Santa Fe Group. This high water-yielding interval is located below the unsaturated volcaniclastic sediments that form the lower portions of the Pliocene Puye Formation, which consists of stratified fanglomerate and conglomerate intervals. These Puye deposits originated from source areas in the Jemez Mountains located to the west, whereas the Santa Fe Group sediments

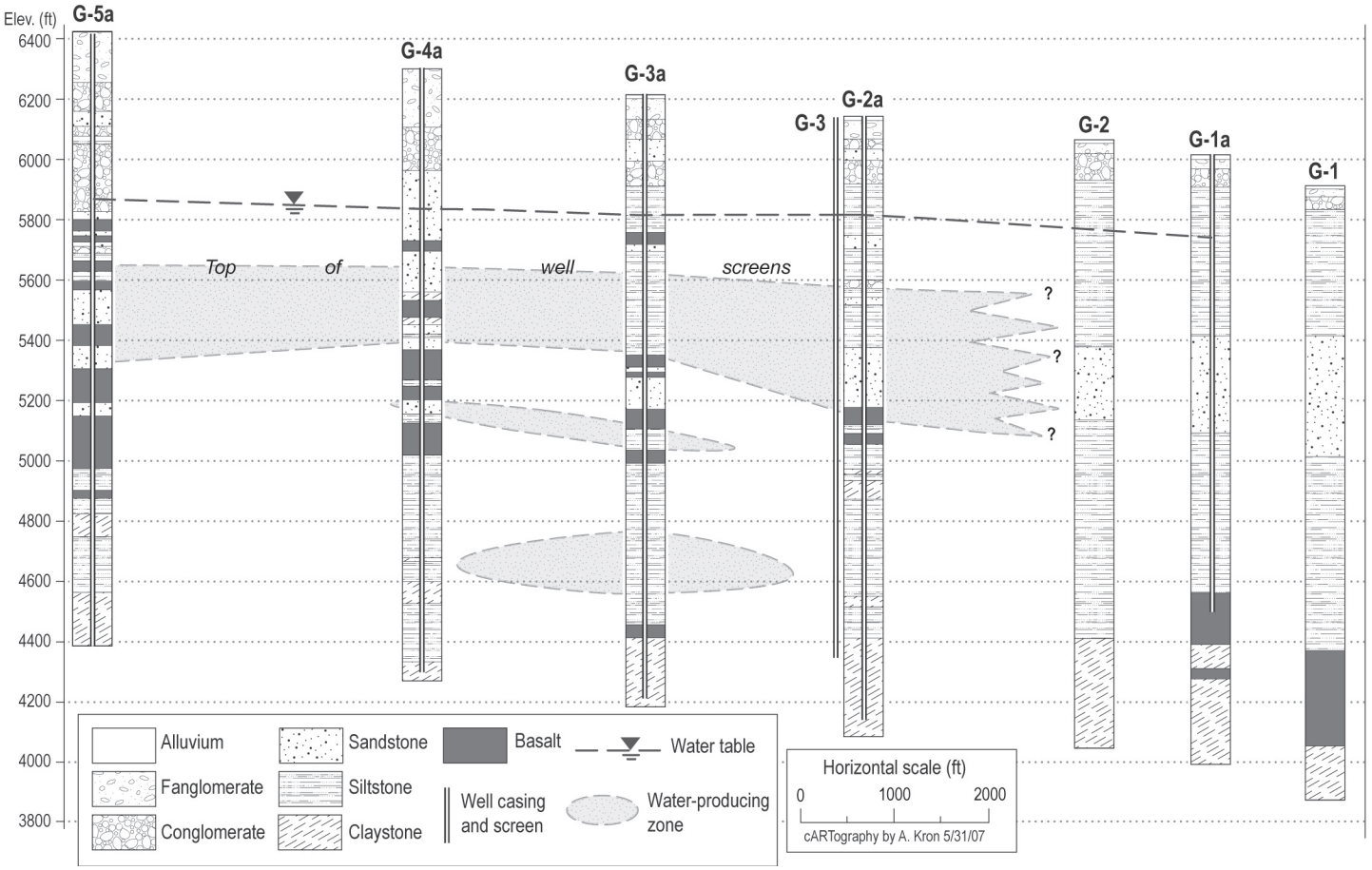

FIGURE 2. Hydrogeological cross-section A-A' following Guaje Canyon. Location of the cross-section is shown in Figure 1. The high-yielding water production zones were defined using flowmeter logs.

originated from source areas located to the north and east of the Española Basin (WoldeGabriel et al., 2006). As implied in Figure 2, the high-yielding zones within the Santa Fe Group are vertically stratified and horizontally discontinuous. More will be said about this later. In the east, these high-yielding zones tend to be located above Miocene basalts, but in the west they are interbedded with them.

Much smaller water volumes are produced from the underlying fine-grained sandstones, siltstones, and claystones that comprise the lower Santa Fe Group. These Santa Fe deposits are overlain by unsaturated portions of Puye fanglomerate and conglomerate in the Guaje well field. While these volcanogenic materials thicken to the west and south, they are not a significant source of water in Guaje Canyon wells. However, in the Guaje well field, the Puye is probably a significant recharge pathway to underlying units. These Puye sediments are saturated farther to the south in the east-central plateau area and comprise some of the most productive units in the regional aquifer. Historical information for the regional aquifer below Pajarito Plateau was previously described by Theis and Conover (1962), Conover et al. (1963), Griggs (1964), and Cushman (1965).

TEST RESULTS

Flowmeter logs

Dynamic, impeller-type, flowmeter logs were obtained for each replacement well and indicate that only a small portion of each well screen yields most of the water to each well (Shomaker, 1999; McLin, 2006b). An example of one of these logs (for well G-2a, Fig. 3) reveals a clear picture of important hydrostratigraphic units. This particular log indicates that Santa Fe Group sediments located immediately below the top of the well screen and down to about 1005 ft below ground surface (bgs) yield almost all of the water produced at this well. These sediments contain five high-yielding zones (zones A, B, C, D, E) that represent only about 325 ft of saturated aquifer material. These zones are located within the 435 ft-thick interval between about 570-1005 ft bgs, and are above the uppermost Miocene basalt layer. This analysis demonstrates that high-yielding zones are sandwiched between thick sequences of lower-yielding sediments. In addition, the high-yielding units are much thinner than the full screen length in each well. While other flowmeter logs are not shown here, they demonstrate that this vertical aquifer heterogeneity is typical throughout the well field. Similar conditions have been documented elsewhere (Izbicki et al., 2005).

Collectively, these flowmeter logs also reveal a water production zone that dramatically thins toward the west (Fig. 2). Since meaningful flowmeter logs can only be recorded in the screened interval of a well, the upper boundary of this high-yielding zone is defined by the contact between the upper solid well casing and lower well screen. The lower boundary is defined according to each flowmeter log since well screens are continuous here. Some water-bearing units may be located above the casing-screen contact in each well, but water must first move vertically downward in the formation or filter pack before entering the well screen. This lack of precise definition for the upper flow-zone boundary implies that the high-yielding zone in the regional aquifer may be thicker than indicated in Figure 2. When this high water producing zone is superimposed onto the geologic cross-section (Fig. 2), it reveals an effective aquifer thickness that cannot be hydraulically characterized by stratigraphy alone. This contrast in hydraulic detail is unrelated to scale effects even though lithology is defined in each well by a 10 ft sampling interval while flowmeter logs are defined by a 0.5 ft sampling interval. Even if geologic samples were collected more often, they would not yield the same information shown in Figure 3.

Aquifer tests

Individual aquifer test results are only briefly discussed here; a detailed analysis and complete data sets are contained in McLin (2006b). Each constant-rate aquifer test consisted of a pumping phase that lasted two days and a non-pumping recovery phase that also lasted two days. Table 1 summarizes important aquifer parameters from these tests. Results from some of the Theis (1935) analyses are graphically shown (Figs. 4-6). Most of these tests reveal pronounced barrier (or no-flow) boundary effects after about 100-400 min of pumping. These boundary effects restrict the radial expansion of the cone of depression outward from the

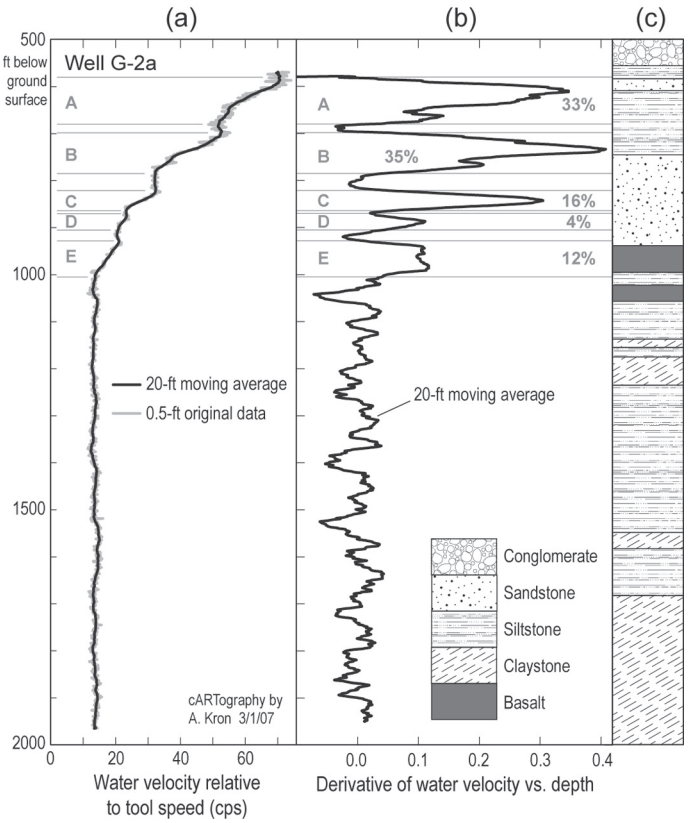

FIGURE 3. Graphical results of the flowmeter log at G-2a showing (a) the velocity log; (b) the derivative of water velocity with respect to depth; and (c) the geologic log opposite the G-2a well screen. Note that (b) shows total water production (%) from individual layers.

TABLE 1. Summary of aquifer parameters from Guaje well field.

Parameter	G-1A[1]	G-2a	G-3a	G-4a	G-5a
Year	1982	1998	1998	1998	1998
***Q* (gpm)**	400	901	800	752	408
***T* (ft²/day)**	4200	3440	1618	1749	700
***S* (dim)**	6.2E-4	9.7E-4	7.7E-4	1.1E-4	6.2E-4
***b* (ft)**	563	435	261	245	325
***K* (ft/day)**	7.5	7.9	6.2	7.1	2.2
S_s **(1/ft)**	1.1E-6	2.2E-6	3.0E-6	4.3E-7	1.9E-6

[1]From specific capacity analysis (McLin, 2006c, 2005b).

pumping well and produce more aquifer drawdown. Each test is briefly discussed below and boundary effects are collectively discussed in the next section.

Graphical results from the G-2a aquifer test are summarized first. Figure 4a shows the curve match between the theoretical Theis type-curve (i.e., the solid line) and observed drawdown (i.e., individual data points) from observation well G-3, while Figure 4b shows simultaneous curve matches for both pumping well G-2a and observation well G-3. These analyses indicate that *T* and *S* estimates from well G-3 are higher than when data from both wells are analyzed together. Recall, however, that the Theis model assumes that *T* and *S* do not change in a homogeneous system. These results suggest that spatial variability in the aquifer response is produced by a combination of head losses near well G-2a and aquifer heterogeneity between the two wells. Drawdown data at G-3 (Fig. 4a) follow the Theis type-curve for about 100-200 min before boundary effects began to dominate (i.e., observed drawdown falls above the Theis type-curve). However, a similar departure occurs after about 400 min in well G-2a, and after about 30 min in G-3 (Fig. 4b). The reported values for *S* in both analyses are characteristic of a confined aquifer response. Some might argue that the results shown in Figure 4a are more reliable because they are from an observation well. Others might favor the results shown in Figure 4b because they are based on data from two wells. We think that both analyses are representative. In addition, we note that a repeat test at well G-2a in 2005 produced *T* and *S* values that were midway between those shown in Figure 4.

All of these observations are important because they reveal slightly different information about the aquifer and wells. First, different results shown in Figure 4 suggest that uncertainty in aquifer parameters may result from alternative methods of analysis. For example, if we compare results shown in Figure 4, we conclude that *T* is about 30% larger using only G-3 data compared to using data from both wells. Parameter uncertainty can be more fully characterized if alternatives to the Theis model are used but this was not done here. Second, the Theis analysis assumes horizontal (radial) flow between the pumping and observation well. This assumption may not hold because the departure times marking the onset of boundary effects are different in each well. Theoretically, these times should be identical. These departure times are different because both *b* and the anisotropy ratio (K_h/K_v) change radially away from well G-2a.

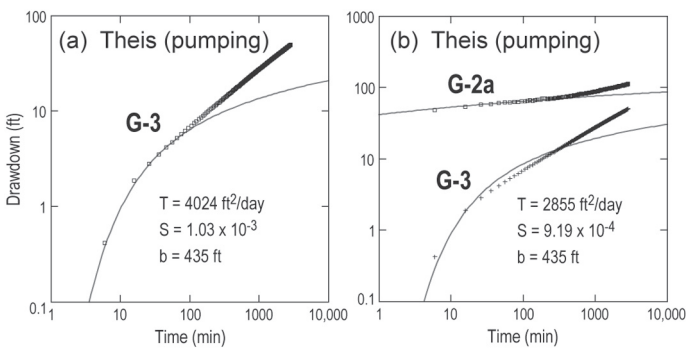

FIGURE 4. Theis aquifer analyses using drawdown data from (a) observation well G-3; and (b) wells G-2a and G-3.

Drilling logs from all of the wells (Fig. 2) suggest that the aquifer is under stratified, water-table (or phreatic) conditions because no single geologic unit can be identified as a confining layer. As previously noted, however, *S* values are characteristic of confined behavior. We note that a layered, phreatic aquifer exhibiting large K_h/K_v ratio differences between layers could respond like a confined system. Conversely, we might also expect a theoretical transition from confined to phreatic behavior to occur. If this transition were actually present in the Guaje system, it was masked by barrier boundary effects that appeared after several hundred minutes. Alternative methods of analysis like those of Neuman (1974) or Moench (1997) consider this transitional behavior but these methods yield similar results to those already shown. Ultimately, the flowmeter logs effectively characterize the aquifer as a vertically stratified system that thins toward to the west. Unfortunately, these logs do not differentiate between a confined or phreatic response so this question remains unanswered. In fact, all of the Guaje Canyon wells contain alternating layers of high and low hydraulic conductivities that are sandwiched together into a single high-yielding, heterogeneous zone that varies both laterally and vertically. At well G-2a, these high-yielding units are located below the unsaturated Puye fanglomerate and above the first Miocene basalts. We note that the barrier boundary effects may be simultaneously related to both aquifer thinning and normal faulting associated with the Rio Grande rift system. These effects are collectively discussed below.

Results from the test at well G-3a are shown in Figure 5. Drawdown and recovery values were again recorded in both pumping well G-3a and observation well G-3. This test differed from the previous one because no boundary effects were observed in G-3a but appeared in well G-3 after about 300 min (Fig. 5). A noticeable decline in *T* between the G-2a and G-3a tests is associated with westward aquifer thinning. In addition, the observed drawdown in G-3 falls below the Theis type-curve (Fig. 5), and suggests a decline in hydraulic communication between wells G-3a and G-3. This barrier boundary response is quite unusual (compare Figs. 4 and 5) and might have been mistaken for a recharge boundary without the flowmeter logs and the G-2a aquifer test. In other words, when the cone of depression radiates westward from well G-2a toward G-3 (Fig. 4a), the barrier boundary causes drawdown to plot above the Theis curve. However, when the cone of depression radiates eastward from well G-3a toward well G-3 (Fig. 5a), the same boundary causes drawdown to plot below the

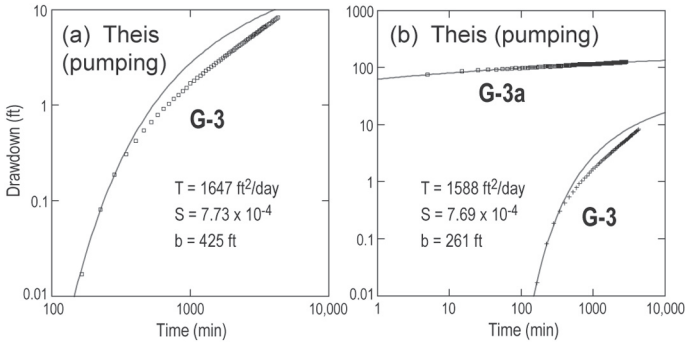

FIGURE 5. Theis aquifer analyses using drawdown data from (a) observation well G-3; and (b) wells G-3a and G-3.

Theis curve. These remarkable observations are probably associated with westward aquifer thinning, directional anisotropy (i.e., the K_h/K_v ratio is higher from east to west than from west to east), and a leaky barrier boundary as discussed below.

Results from the test at well G-4a are shown in Figure 6. Again, drawdown and recovery were recorded in both pumping well G-4a and observation well G-4. The most significant result from this test is that T values are comparable to those at well G-3a. As seen in Table 1, K values are remaining about the same between wells G-3a and G-4a because the aquifer thickness declines only slightly. Some drawdown effects in G-4a are caused by a barrier boundary but these effects are absent in well G-4. These observations suggest that the boundary near well G-4a may be different than the multiple boundary effects seen near wells G-2a and G-3. More will be said about this later.

Graphical results from the G-5a test are not shown here. This test is still noteworthy because it showed no drawdown response at observation wells G-4a and G-4 while G-5a was pumped. These results also indicate that T is only about 700 ft^2/day, and that significant boundary effects appear in G-5a after 100-200 min of pumping. Since the cone of depression did not intersect an observation well, a reliable estimate for S could not be made.

Barrier boundary effects

Boundary effects were observed in wells G-2a, G-3, G-4a, and G-5a but not in G-3a and G-4 (Figs. 1, 4-6). The importance of this sequence will become clear later. Despite the unusual response for well G-3 (Fig. 5), all of these boundaries represent barriers to flow. These effects can be analyzed using traditional image well theory (e.g., Walton, 1970). For example, the G-3 boundary influences shown in Figure 4a begin after 100-200 min of pumping at G-2a. In addition, the almost linear appearance of the boundary effect is striking (i.e., the drawdown appears like a straight line after 100 min). If only one boundary were present, we would not expect to see this type of response. We conclude that more than one boundary is affecting drawdown at well G-3. In addition, boundary effects appear at different times in G-3 and G-2a (Fig. 4). Normally we expect the expanding cone of depression to radiate quickly from the production well. Hence, the first appearance of a boundary should be similar in both G-3 and G-2a. The significant timing difference in this first appearance suggests that the aquifer is heterogeneous. This observation is also consistent with the G-2a flowmeter log (Fig. 3). The multiple boundary effects seen at G-3 are probably associated with both aquifer thinning and buried faults between wells; faulting based on lithology was described by WoldeGabriel et al. (2006). We can analyze the first of several boundary effects by starting with the T and S values shown in Figure 4a and the image well analysis described by Walton (1970). This analysis says that the first boundary must be located about 600 ft away from well G-3. With only one observation well, however, it is apparent that we can not precisely locate the first boundary or determine its orientation.

If we combine this image well analysis with other geologic information, we may still be able to identify the nature and approximate locations of several boundaries. Projections of several normal faults were extended into the Guaje well field for this analysis (Fig. 7). These faults were previously mapped by Dethier (2003) but he could not detect them in the alluvial canyon fill. While several fault projections pass near wells G-3 and G-2a, all of these are located much farther away than 600 ft. We conclude that the initial G-3 boundary effect (Fig. 4) cannot be associated with any of these projections, but they may account for subsequent effects as described below. The early linear drawdown behavior in G-3 is more likely related to aquifer thinning between wells G-2a, G-3 and G-3a. This thinning is clearly shown in Figure 2 and is based on flowmeter logs from each well. Fault Projections 1 and 2 (Fig. 7) are optimally located so that they could account for secondary and tertiary boundary effects recorded at both G-3 and G-2a.

All of the fault projections shown in Figure 7 are intriguing because they can account for complex, multiple boundary effects in several wells. The first projection is located about 1200 ft east of well G-2a and passes between wells G-2a and G-1a. This is important because no drawdown was recorded in well G-1a during a repeat aquifer test at G-2a in 2005 (McLin, 2006b). According to T and S values shown in Table 1, pumping at G-2a should produce drawdown at G-1a. The presence of a barrier boundary represented by this fault projection would explain this lack of observed drawdown. It would also account for secondary and tertiary boundary effects at G-2a and G-3 (Fig. 4). The delayed timing departures marking the onset of multiple boundary effects (Figs. 4, 5) also appear to be affected because Fault Projection 1

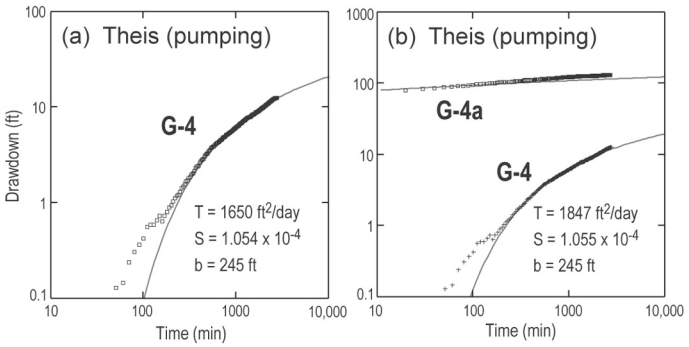

FIGURE 6. Theis aquifer analyses using drawdown data from (a) observation well G-4; and (b) wells G-4a and G-4.

is located farther away from G-2a than Fault Projection 2. This second projection passes between wells G-3 and G-3a and would explain the poor hydraulic communication noted in Figure 5. This same projection also accounts for the poor communication between wells G-2a, G-3a, and G-4a during the 2005 repeat test. This poor hydraulic communication suggests that Fault Projection 2 is actually a leaky barrier boundary. Finally, Projection 3 passes between wells G-4a and G-5a. This last projection would explain why there is such a dramatic reduction in *K* values between these two wells and why there are boundary effects at both G-4a and G-5a. In addition, it would account for the lack of observed drawdown at G-4a when G-5a was pumped.

No boundary effects were seen in well G-4 (Fig. 6b), but a relatively subdued barrier boundary effect was present in well G-4a. This effect is also smaller than those at wells G-2a and G-3. In fact, multiple boundary effects appear to diminish toward the west because drawdown values associated with different boundaries are systematically smaller in each respective aquifer test. The corresponding *T* values also decline in this same direction. This declining influence coincides with westward aquifer thinning that was noted earlier even though *K* values remain relatively constant. Changes in *b* between wells G-3a, G-4a, and G-5a are relatively small (Fig. 2). In fact, boundary effects disappear at well G-3a and G-4 and then reappear at wells G-4a and G-5a. This disappearance suggests that the primary boundary effects at wells G-2a and G-3 are associated with aquifer thinning and that secondary effects are associated with Fault Projection 2 (Fig. 7). Fault Projection 1, on the other hand, appears to be related to tertiary boundary influences at both G-2a and G-3. The reappearance of boundary effects at wells G-4a and G-5a suggests that these latter wells are primarily affected by Fault Projection 3 rather than changes in *b*. In addition, slight aquifer thickening between G-4a and G-5a may have produced secondary effects at both wells. This interpretation is supported by the relatively small barrier boundary effect seen in well G-4a, and the somewhat larger boundary effect that appeared in the G-5a test (McLin, 2006b). Furthermore, the corresponding *T* value near G-5a declines sharply from those noted earlier for G-3a and G-4a. This sharp decline is also reflected in the corresponding *K* values reported in Table 1.

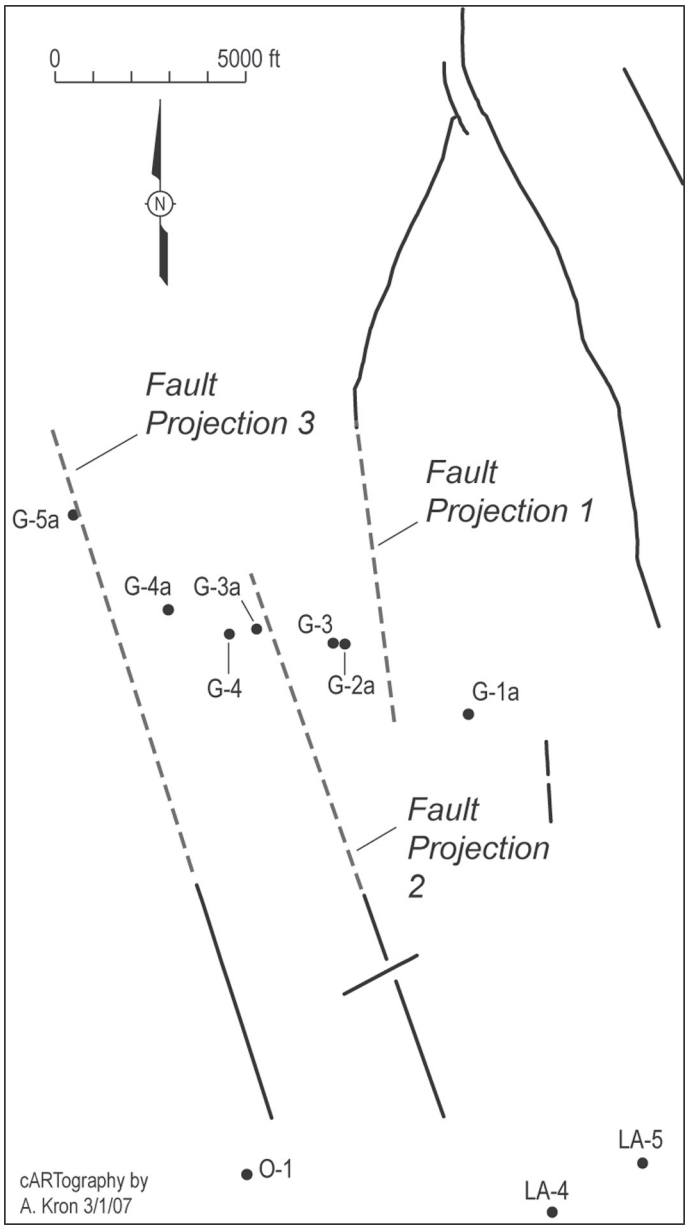

FIGURE 7. Solid lines represent locations of previously mapped faults (Dethier, 2003). Dashed lines are fault projections identified in aquifer tests presented here.

Finally, the subparallel orientations of the fault projections (Fig. 7) are crucial in understanding recharge in the Guaje system. According to image well theory, this configuration can generate complex drawdown effects because expanding cones of depression are distorted when they reflect off each barrier boundary. In Guaje Canyon, we have northwest-southeast trending aquifer slabs between subparallel faults and a well field that is oriented east-southeast across these slabs. If each fault responds like a barrier boundary to pumping, then individual aquifer slabs are hydraulically isolated from one another. If fault boundaries are leaky, then there is hydraulic communication between slabs. Hence, the hydraulic nature of these boundaries may alter the spatial distribution of well-field capture zones and potentially modify recharge pathways to individual wells.

CONCLUSIONS

The sequential aquifer tests described here are significant for several reasons. First, these tests recorded drawdown and recovery data that can be used to evaluate important aquifer parameters (Table 1). These tests are supplemented by dynamic flowmeter logs that accurately define thickness variations in high-yielding aquifer units between wells. They also demonstrate that screen length is not a good representation for aquifer thickness. These logs show that the most productive units are located above the first Miocene basalt flows in the eastern portions of the Guaje well field, and are interbedded with the basalts in the west. These highly transmissive zones generally correspond to piedmont-derived fluvial sediments within the upper Miocene Santa Fe Group that have an eastern or northern source area. The sand-

stones, siltstones, and claystones located below the basalts yield relatively little water to Guaje wells (Fig. 3). This behavior is typical of the Tesuque Formation (Santa Fe Group) throughout most of the Española Basin.

Secondly, these sequential aquifer tests have clearly identified a dramatic reduction in *T* values between well G-2a on the east and well G-5a on the west. This dramatic change is strongly correlated to an equally dramatic thinning of the high-yielding aquifer units between these same wells (Fig. 2). These observations demonstrate that the aquifer is vertically stratified and horizontally discontinuous below this portion of Guaje Canyon. In addition, the reported values for *S* are characteristic of a confined aquifer response.

Finally, the observed changes in *T* are also related to normal faulting that was revealed during sequential aquifer testing. Three buried faults pass through the Guaje well field and create extraordinary responses to pumping. When combined with westward aquifer thinning, complex multiple barrier boundary effects are produced that reveal anisotropy in an unusual way. These observations suggest a very different hydrogeologic picture from that in the central plateau region (McLin, 2005a, 2006a). As seen in Figure 7, the first buried fault is located about 1200 ft east of well G-2a. The second one passes between wells G-3 and G-3a, and a third fault is located between wells G-4a and G-5a. Drawdown observations also imply that some barrier boundaries may be leaky (e.g., Fault Projection 2) while others are not (e.g., Fault Projections 1 and 3).

ACKNOWLEDGMENTS

Portions of this work were supported by the Environmental Stewardship Division at Los Alamos National Laboratory (LANL). Special thanks are extended to Timothy Glasco, Deputy Utility Manager, and Wayne Witten, Water System Superintendent, Department of Public Utilities, County of Los Alamos, for their support and cooperation during the 2005 aquifer test at well G-2a. This manuscript also benefited greatly from comments and suggestions provided by Bruce Gallaher and David Rogers at LANL. The LANL number for this document is LA-UR-07-1424.

REFERENCES

Broxton, D.E., and Reneau, S.L., 1996, Buried early Pleistocene landscapes beneath the Pajarito Plateau, northern New Mexico: New Mexico Geological Society, 47th Field Conference, Guidebook, p. 325-334.

Broxton, D.E., and Vaniman, D.T., 2005, Geologic framework of a groundwater system on the margin of a rift basin, Pajarito Plateau, north-central New Mexico: Vadose Zone Journal, v. 4, p. 522-550.

Collins, K.A., Simmons, A.M., Robinson, B.A., and Nylander, C.L., eds., 2006, Los Alamos National Laboratory's hydrogeologic studies of the Pajarito Plateau, a synthesis of hydrogeologic work plan activities, 1998-2004: Los Alamos National Laboratory, Report LA-14263-MS.

Conover, C.S., Theis, C.V., and Griggs, R.L., 1963, Geology and hydrology of the Valle Grande and Valle Toledo, Sandoval County, New Mexico: U. S. Geological Survey, Water Supply Paper 1619-Y, 37 p.

Cushman, R.L., 1965, An evaluation of aquifer and well characteristics of municipal well fields in Los Alamos and Guaje Canyon near Los Alamos, New Mexico: U. S. Geological Survey, Water Supply Paper 1809-D, 50 p.

Dethier, D.P., 2003, Geologic map of the Puye Quadrangle, Los Alamos, Rio Arriba, Sandoval, and Santa Fe Counties, New Mexico: U. S. Geological Survey, Miscellaneous Field Studies Map MF-2419, scale 1:24,000.

Fetter, C.W., 1994, Apllied Hydrology. 3rd edition: New Jersey, Prentice-Hall, 691 p.

Griggs, R.L., 1964, Geology and ground-water resources of the Los Alamos area, New Mexico: U. S. Geological Survey, Water Supply Report 1753, 107 p.

Izbicki, J.A., Christensen, A.H., Newhouse, M.W., Smith, G.A., and Hanson, R.T., 2005, Temporal changes in the vertical distribution of flow and chloride in deep wells: Ground Water, v. 43, p. 531-544.

McLin, S.G., 2005a, Analysis of the PM-2 aquifer test using multiple observation wells: Los Alamos National Laboratory, Report LA-14225-MS.

McLin, S.G., 2005b, Estimating aquifer transmissivity from specific capacity using Matlab: Ground Water, v. 43, p. 611-614.

McLin, S.G., 2006a. Analysis of the PM-4 Aquifer Test Using Multiple Observation Wells: Los Alamos National Laboratory, Report, LA-14252-MS.

McLin, S.G., 2006b, Analysis of sequential aquifer tests from the Guaje well field: Los Alamos National Laboratory, Report LA-UR-06-2494.

McLin, S.G., 2006c, A catalog of historical aquifer tests on Pajarito Plateau: Los Alamos National Laboratory, Report LA-UR-06-3789.

Moench, A.F., 1997, Flow to a well of finite diameter in a homogeneous, anisotropic, water table aquifer: Water Resources Research, v. 33, p. 1397-1407.

Neuman, S.P., 1974, Effect of partial penetration on flow in unconfined aquifers considering delayed gravity response: Water Resources Research, v. 10, p. 303-312.

Purtymun, W.D., 1984, Hydrologic characteristics of the main aquifer in the Los Alamos area; development of ground water supplies: Los Alamos National Laboratory, Report LA-9957-MS.

Purtymun, W.D., 1995, Geologic and hydrologic records of observation wells, test holes, test wells, supply wells, springs, and surface water stations in the Los Alamos area: Los Alamos National Laboratory, Report LA-12883-MS.

Purtymun, W.D., and Stoker, A.K., 1988, Water supply at Los Alamos; current status of wells and future water supply: Los Alamos National Laboratory, Report LA-11332-MS.

Purtymun, W.D., and Johansen, S., 1974, General geohydrology of the Pajarito Plateau: New Mexico Geological Society, 25th Field Conference, Guidebook, p. 347-349.

Reneau, S.L., and Dethier, D.P., 1996, Pliocene and Quaternary history of the Rio Grande, White Rock Canyon and vicinity, New Mexico: New Mexico Geological Society, 47th Field Conference, Guidebook, p. 317-324.

Shomaker, J., 1999, Well report; construction details and testing, Guaje replacement wells GR-1, GR-2, GR-3, and GR-4, Santa Fe County, New Mexico: Private consulting report to Los Alamos National Laboratory, John Shomaker and Associates, Inc., Albuquerque, NM.

Theis, C.V., 1935, The relation between the lowering of the piezometric surface and the rate and duration of discharge of a well using groundwater storage: American Geophysical Union Transactions, v. 16, p. 519–524.

Theis, C.V., and Conover, C.S., 1962, Pumping tests in the Los Alamos Canyon well field near Los Alamos, New Mexico: U.S. Geological Survey, Water Supply Paper 1619-I, p. 24.

Walton, W.C., 1970, Groundwater Resource Evaluation: New York, McGraw-Hill Book Company, 664 p.

WoldeGabriel, G., Warren, R.G., Chipera, S., and Keating, E., 2006, Geological characteristics of the Guaje Canyon well field in the Pajarito Plateau of the Española Basin, Rio Grande rift: Los Alamos National Laboratory, Report LA-11332-MS.